Parametric Identification of DQ Impedance Model for Three-Phase Voltage-Source Converters

Hong, Gong; Yang, Dongsheng; Wang, Xiongfei

Published in:
Proceedings of the 2018 IEEE International Power Electronics and Application Conference and Exposition, PEAC 2018

DOI (link to publication from Publisher):
10.1109/PEAC.2018.8590653

Publication date:
2018

Document Version
Accepted author manuscript, peer reviewed version

Parametric Identification of DQ Impedance Model for Three-Phase Voltage-Source Converters

Hong Gong, Dongsheng Yang, Xiongfei Wang
Department of Energy Technology
Aalborg University
Aalborg, Denmark
hgo@et.aau.dk, doy@et.aau.dk, xwa@et.aau.dk

***Abstract*—The impedance-based approach has been widely used to predict the system stability at each point of connection of the individual voltage-source converter (VSC). However, the analytical impedance model is difficult to obtain because the system operators usually have no access to the detailed data of the control system of power converters due to confidentiality of manufacturers. Therefore, impedance measurement is necessary. In this paper, a broadband signal, pseudo-random binary sequence (PRBS) is selected as injected perturbations to excite the voltage and current response of VSC. Moreover, a parametric identification method for impedance measurement of VSC in the *dq*-frame is proposed based on recursive least squares algorithm. According to the nonlinear time-domain simulation data and the experimental data, the identified model of the converter is obtained. The accuracy of this impedance measurement method based on the parametric identification is verified in both the time-domain and frequency-domain.**

Keywords—Parametric identification, DQ impedance model, impedance measurement, PRBS, VSC

I. INTRODUCTION

The impedance-based stability analysis method has been widely applied for stability analysis since it does not need to systematically formulate the state-space models of the whole system, and predict the system stability based on the ratio of the output impedance of VSC to the equivalent system impedance [1], [2]. However, the analytical impedance model is difficult to obtain since system operators have no access to the detailed data of the control system of power converters. Thus, there is a huge demand for the impedance measurement.

The DC impedance measurement technology is mature and widely available in the power system[3], [4]. Nevertheless, in the case of three-phase AC systems, since there is no equilibrium dc operating point for the small-signal linearization, the small-signal impedance model of converter is developed in the rotating *dq*-frame to analyze the dynamic interactions between the grid-connected converters and grid impedance [5].

In recent years, several approaches have been proposed for measuring the output impedance of the three-phase converters in the *dq*-frame [6]-[9]. A common approach is to inject single-frequency excitation signal at one time, and calculate the magnitude and phase of the impedance at that frequency [6], [7]. However, multiple experiments must be carried out to obtain the impedance in a wide frequency range. Another way is based on broadband excitation signals, such as an impulse or PRBS, and the impedance characteristic can be calculated by performing the Fast Fourier Transformation (FFT) on the measured voltage and current at one time [8], [9]. However, the measured impedance models obtained from above-measured methods are non-parametric models, which only represents the frequency response of the converter at the specific frequency point. They are not suitable for the system-level simulation analysis and controller design [10]. Moreover, non-parametric identification method has to be implemented with a large amount of recorded data by using FFT, which may not be suitable for measuring the impedance online and monitoring the change of the system status and parameters in the real time due to the limitation of the memory. In order to address these issues, parametric impedance model is obtained in [11]-[14]. With the help of recursive algorithms, the parametric identification method can be achieved by using less data and much lower requirements of software's and hardware's configuration. Based on the frequency response measured at the converter terminals, the polytopic black-box model of DC-DC converters is developed for system-level design and analysis in [11], [12]. According to the transient response of the voltage and current of the converter to the passive load step, a parametric black-box model technique is proposed in [13], [14]. Nevertheless, the frequency range of the perturbations caused by the load step cannot controlled while controlled perturbations such as PRBS provide better control and ease the measurement task. Moreover, the load step may change the operating point of the system, which may influence the accuracy of the impedance measurement results.

In order to obtain the parametric impedance model of VSC in the *dq*-frame by measurement, this paper propose the use of PRBS as injected perturbations to excite the response of the converter. According to the measured voltages and currents, the identified impedance model of converter is obtained based on the recursive least squares algorithm. The accuracy of the identified model is verified in both the time-domain and frequency-domain.

II. SMALL-SIGNAL IMPEDANCE MODEL OF VSC

Fig.1 (a) shows an example of three-phase VSC used to illustrate the concept of impedance model. L and R are filtered inductor and its parasitic resistor, respectively. I_{abc} and U_{abc} represent three-phase currents of converter and PCC voltages, respectively. U_{dc} denotes the dc voltage and θ is the synchronization phase angle generated by PLL. $\mathbf{Z_{dq}}$ is the dq impedance matrix of the converter, which models all circuit components, including physical components and control systems. Fig.1 (b) shows the small-signal output impedance model of the converter in the *dq*-frame. The purpose of the the impedance measurement is to obtain analytical expression of Z_{dd}, Z_{qq}, Z_{dq}, Z_{qd}.

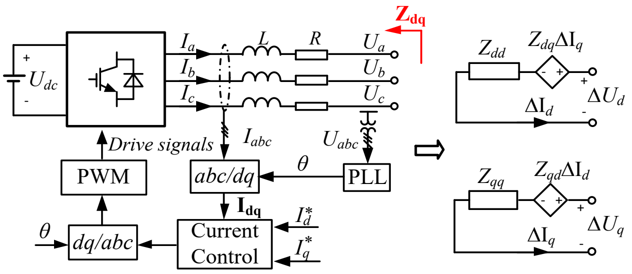

(a) (b)

Fig.1. Equivalent circuit diagram of VSC.

For the balanced and symmetrical three-phase AC system, the dq impedance model is widely used because there exist dc operation point in the dq-frame. Similar to DC systems, the relationship between small variations of dq-axis voltages and currents can be applied for describing the dq impedance characteristic of converters. Thus, the small-signal dq impedance model of converters can be derived by linearizing voltages and currents around its steady-state operating point, as shown in (1).

$$\begin{bmatrix} \Delta U_d \\ \Delta U_q \end{bmatrix} = \mathbf{Z_{dq}} \begin{bmatrix} \Delta I_d \\ \Delta I_q \end{bmatrix} = \begin{bmatrix} Z_{dd} & Z_{dq} \\ Z_{qd} & Z_{qq} \end{bmatrix} \begin{bmatrix} \Delta I_d \\ \Delta I_q \end{bmatrix} \tag{1}$$

where $\triangle$ denotes a small-signal variation of the respective variables from the equilibrium point.

Since the VSC is operating as a current source, the impedance is presented as an admittance, which can be calculated as (2).

$$\begin{bmatrix} \Delta I_d^m \\ \Delta I_q^m \end{bmatrix} = \mathbf{Y_{dq}} \begin{bmatrix} \Delta U_d^m \\ \Delta U_q^m \end{bmatrix} = \begin{bmatrix} Y_{dd} & Y_{dq} \\ Y_{qd} & Y_{qq} \end{bmatrix} \begin{bmatrix} \Delta U_d^m \\ \Delta U_q^m \end{bmatrix} \tag{2}$$

III. Impedance Measurement Technology in the DQ-Frame

In order to measure the impedance model of VSC in the dq-frame, the corresponding system diagram of the impedance measurement setup is proposed, as shown in Fig.2. In this setup, PRBS is chosen as the excitation signal. U_d^p, U_q^p represent the designed excitation signal in the dq-frame U_{abc}^p represents the actually injected three-phase voltage perturbations. I_d^m, I_q^m, U_d^m and U_q^m denote the measured current and voltage of the converter in the dq-frame, respectively, which are applied for the identification of the impedance model of the converter.

In general, in order to acquire the specific components of the impedance matrix as shown in (1) and (2), two linearly independent perturbations are required to gain enough information. The excitation signal with the frequency of interest is firstly generated on the d-axis while the q-axis perturbation is equal to zero. Similarly, a second perturbation sequence is implemented but injecting the q-axis perturbation instead, with the d-axis components being zero. In this case, the proposed identification method considers that only one input signal is perturbed on the one axis while the disturbance on the other axis is negligible.

Therefore, when the voltage excitation signal is superposed to the d-axis, the responses of current ΔI_d and ΔI_q are

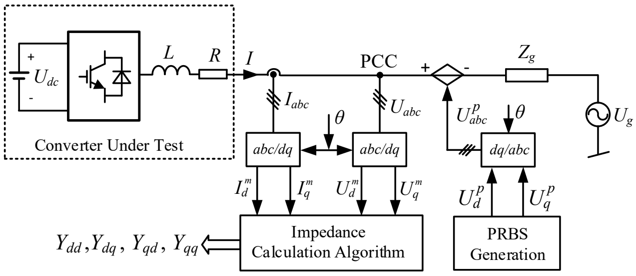

Fig.2. System diagram of the impedance measurement setup.

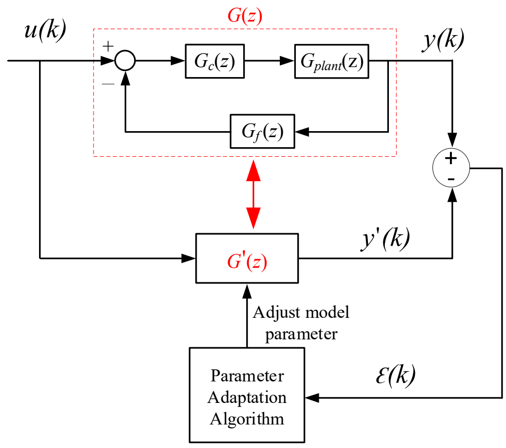

Fig.3. Basic principle of model identification.

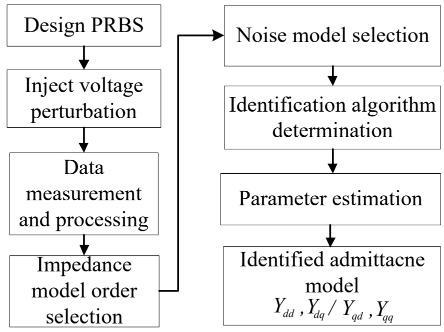

Fig.4. Flowchart of the identification procedure.

caused by ΔU_d and the admittance Y_{dd}, Y_{qd} could be identified as expressed in (5)

$$Y_{dd} = \left. \frac{\Delta I_d^m}{\Delta U_d^m} \right|_{\Delta U_q^m = 0}, \qquad Y_{qd} = \left. \frac{\Delta I_q^m}{\Delta U_d^m} \right|_{\Delta U_q^m = 0} \tag{3}$$

Similarly, the admittance Y_{dq}, Y_{qq} could be identified as expressed by

$$Y_{dq} = \left. \frac{\Delta I_d^m}{\Delta U_q^m} \right|_{\Delta U_d^m = 0}, \qquad Y_{qq} = \left. \frac{\Delta I_q^m}{\Delta U_q^m} \right|_{\Delta U_d^m = 0} \tag{4}$$

According to the input and output data, the expression of (3), (4), namely the transfer function of the admittance, could easily obtain based on the parametric identification method. The purpose of the parametric identification is to find an appropriate model $G'(s)$ whose output (current) fitting very well with the output of the actual model $G(s)$ under the same input (voltage), as shown in Fig.3. Based on the parameter adaptation algorithm as well as the error between the actual model and identified model, the parameters of the identified model are adjusted constantly until meeting the requirements of the precision. The detailed explanation will be given in the following section.

IV. Impedance Measurement Procedure based on Parametric Identification

Fig.4 shows the flowchart of the impedance measurement based on parametric identification, which consists of excitation signals design, selection of model structure, determination of model order and identification algorithm.

A. Design of Excitation Signals

In order to identify the impedance over a wide frequency range and save the measurement time, a broadband excitation signal should be chosen. PRBS is a periodic signal whose period is defined by the length of the sequence L, which has spectral content rich in frequencies [15]. Although PRBS can be easily generated by using shift register with feedback, the specific generation is dependent on the test time and the dynamic character of the model to be identified. Therefore, the excitation signals have to be carefully designed.

To obtain the response of VSC over the entire frequency spectrum generated by a particular PRBS, the test time should be larger than at least one period of PRBS. Besides, the maximum duration of a pulse of PRBS would influence the accuracy of identified model's steady gain, which is mainly because the excitation signal should assure at least one completed dynamic response of the system before the next excitation signal comes. However, the resolution of the PRBS is generally chosen low enough to satisfy this need.

What's more, the choice of the magnitude of PRBS is very important, e.g., when the magnitude of PRBS is smaller than the residual noise, the excitation signal would submerge in the noise and might obtain an inaccurate model. On the other hand, when the magnitude of PRBS is very large, it is likely to excite the non-linear character of the model to be identified. Therefore, the magnitude of PRBS should be chosen in the reasonable level. In this paper, the small-signal impedance model would be identified, which means the magnitude of PRBS should be determined based on the steady operating point.

B. Selection of Model Structure

Before the identification, the specific structures of the identified model should be determined. The general structure of the transfer function model, identified through parametric methods, is given by (5), where $u(k)$ and $y(k)$ are measured system input and output, respectively. $A(z^{-1})$ and $B(z^{-1})$ are the polynomial of output and input, whose coefficients are parameters required to be identified. $H(z^{-1})$ is named as disturbance polynomial and $d(k)$ is white noise. As can be noticed, since the identified model is acquired based on sampling data, a discrete model is identified.

$$A(z^{-1})y(k) = B(z^{-1})u(k) + H(z^{-1})d(k) \tag{5}$$

In particular, when the disturbance input is the white noise, the noise transfer function $H(z^{-1})$ also exists several forms. This is mainly because there is no general model structure that could describe all the situations encountered in practical cases. In this paper, the disturbance input is considered as the white noise and the noise transfer function $H(z^{-1})$ is chosen as 1 since the measured input and output data would be preprocessed first before it is used for identification. Therefore, the identification would be easier to implement and the model order is simpler.

C. Determination of Model Order

The next step is to select the order of the polynomials $A(z^{-1})$ and $B(z^{-1})$. Traditionally, trial and error could be used to determine the model order, and the fitting performance between the actual model and identified model would be checked. If the identified model could not satisfy the dynamic character of the actual model, the model order would be selected again. If we increase the order of the polynomials, it will increase the computational complexity and on the other hand, if we reduce the order, the accuracy of the estimated model will compromised. There is a trade-off between computational complexity and accuracy of the identified impedance model.

D. Identification Algorithm

The key part of parametric identification is the identification algorithm. The parameters of the identified model, given by (5), would obtain by minimizing the objective function. General choices are to minimize the sum of squared prediction error J_1, given by the following equations

$$minJ_1 = \frac{1}{N}\sum_{i=1}^{N}[\varepsilon^0(i)]^2 \tag{6}$$

where N is the number of samples, $\varepsilon^0(i)$ is the prediction error between the actual model and identified model.

This minimization of (6) could be easily implemented by some software using existed identification algorithm. In this paper, the recursive least squares algorithm was applied to identify the parameters of the model that optimize the objective function J_1. The detailed parameter adaptation algorithm is given by

$$\hat{\theta}(k+1) = \hat{\theta}(k) + F(k+1)\phi(k)\varepsilon^0(k+1) \tag{7}$$

$$F(k+1) = F(k) - \frac{F(k)\phi(k)\phi(k)^T F(k)}{1+\phi(k)F(k)\phi(k)} \tag{8}$$

where $\hat{\theta}(k)$ is the estimated parameters vector, i.e. the coefficient of polynomials $A(z^{-1})$ and $B(z^{-1})$. $F(k)$ is the adaptation matrix gain. $\phi(k)$ is the vector of measured data, i.e. current and voltage of converter.

The selection of the adaptation gain would determine the quality of the identification algorithm, e.g., when the parameters are close to the optimum, high adaptation gain may bring about oscillations around the minimum, while when the estimated parameters are far from the optimum, higher adaptation gain would obtain faster convergence speed. Therefore, accordingly varied adaptation gain is desired. As can be found in (8), the adaptation gain $F(k)$ in the identification algorithm adopted in this paper is time varying which is associated with the measured data.

In order to obtain a different variation profile of the adaptation gain applying for different situations, two weighting functions $\beta_1(k)$ and $\beta_2(k)$ are introduced. Formula (8) could be rewritten as

$$F(k+1) = \frac{1}{\beta_1(k)}F(k) - \frac{F(k)\phi(k)\phi(k)^T F(k)}{\dfrac{1}{\beta_2(k)} + \dfrac{\phi(k)F(k)\phi(k)}{\beta_1(k)}} \tag{9}$$

TABLE I. PARAMETERS OF THE CONVERTER UNDER TEST

Symbol	Description	Value
K_{i_p}/K_{i_i}	Current inner controller	7.85/274
K_p/K_i	PI controller of PLL	0.24/4.44
ω	Grid frequency	314 rad/s
f_s	Sampling frequency	10 kHz
I_{d0}	d channel current steady value	8 A
I_{q0}	q channel current steady value	0 A
U_{d0}	d channel voltage steady value	202 V
U_{q0}	q channel voltage steady value	0 V
U_{dc0}	DC voltage of converter	730 V
U_g	Grid phase-ground peak voltage	220 V
L	Filtered inductor	3 mH
C_g	Grid capacitor	20 μF
L_g	Grid inductor	17 mH

Different selection of $\beta_1(k)$ and $\beta_2(k)$ could obtain different feature of the adaptation gain which might be suitable for the identification of different systems. In this paper, constant $\beta_1(k)$ and $\beta_2(k)$ are both given by 1. The reason why chooses this form of weighting function is that in this paper, the system to be identified assumes to have constant parameters and the original form of the adaptation gain is able to meet the requirements.

V. SIMULATION AND EXPERIMENT VALIDATION

A. Simulation Validation

The simulation model of VSC was established in MATLAB/Simulink based on Fig.1 and the corresponding measurement model was built according to Fig.2. The specific parameters of VSC are shown in Table I.

According to the simulation data, the transfer functions of the identified impedance model are given in the following. For the sake of simplicity, the lowest order that provides a good fit has been selected.

$$Y_{dd}=\frac{-0.01647z^{-1}+0.006874z^{-2}+0.01192z^{-3}-0.002327z^{-4}}{1-1.464z^{-1}-0.04418z^{-2}+0.6729z^{-3}-0.1644z^{-4}}$$

$$Y_{dq}=\frac{-0.0005z^{-2}+0.0012z^{-3}-0.00062z^{-4}}{1-3.64z^{-1}+4.954z^{-2}-2.987z^{-3}+0.673z^{-4}}$$

$$Y_{qd}=\frac{0.00024z^{-1}+0.0012z^{-2}-0.00036z^{-3}}{1-2.69z^{-1}+2.4z^{-2}-0.711z^{-3}}$$

$$Y_{qq}=\frac{0.004-0.08z^{-1}+0.068z^{-2}+0.059z^{-3}-0.01z^{-4}-0.036z^{-5}}{1-0.84z^{-1}-1.44z^{-2}+0.96z^{-3}+0.74z^{-4}-0.43z^{-5}}$$

Fig.5~ Fig.8 show the comparison of the admittance between the calculated results through the theoretical impedance model and the identified impedance model. All the impedance were measured from 1Hz to 1000Hz. As can be seen, the admittance Y_{dd} and Y_{qq} obtained from the theoretical calculation and identification match very well in the wide frequency range. However, the coupling admittance Y_{dq} and Y_{qd} exist small difference in the low frequency range (below 3Hz). This is mainly because the magnitude of the transfer function of the coupling admittance is too small and small perturbations cannot excite enough response of VSC. Nevertheless, this difference will not influence the stability analysis results because the magnitudes of the coupling impedance Y_{dq} and Y_{qd} in the low frequency range are relatively small compared with Y_{dd} and Y_{qq}.

Furthermore, the processed output currents of the identified and simulated model under two different injected voltage perturbations are compared in Fig.6. As can be seen, the output current of the identified model of Y_{dd} and Y_{qq} match the actual model output very well (96.5% and 97% respectively) while the output of the identified coupling impedances Y_{dq} and Y_{qd} show small mismatch (78% and 87%), which draws the same conclusion as the frequency-domain results.

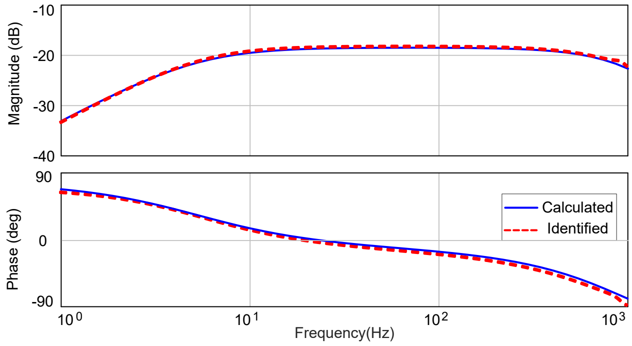

Fig.5. Theoretically calculated admittance and identified admittance of Y_{dd}.

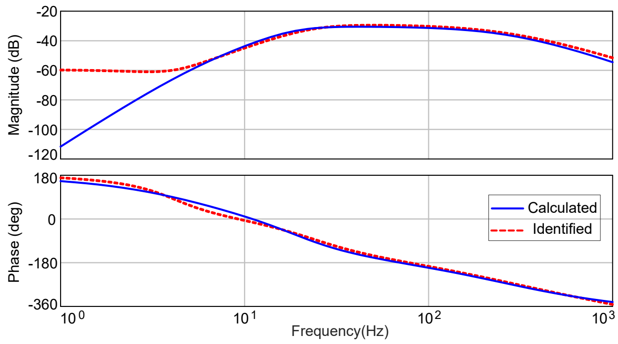

Fig.6. Theoretically calculated admittance and identified admittance of Y_{dq}.

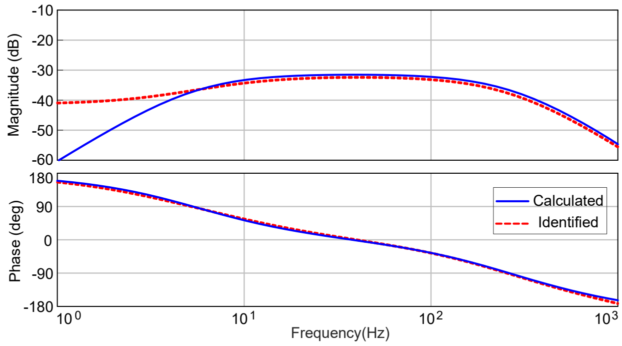

Fig.7. Theoretically calculated admittance and identified admittance of Y_{qd}

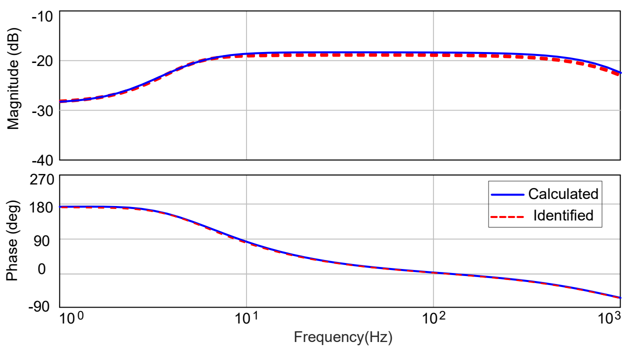

Fig.8. Theoretically calculated admittance and identified admittance of Y_{qq}.

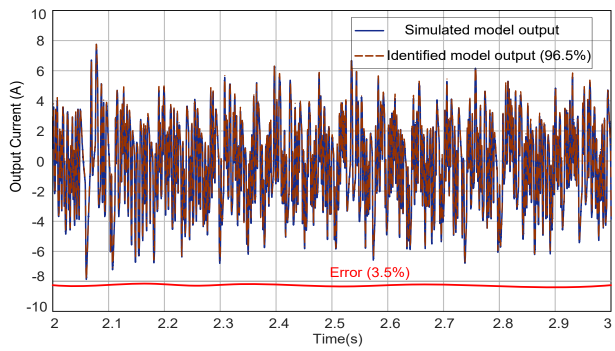

Fig.9. D-axis current outputs of simulation and identified model under the D-axis voltage excitation

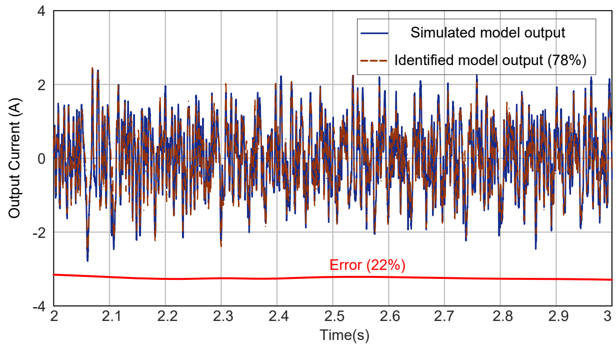

Fig.10. Q-axis current outputs of simulation and identified model under the D-axis voltage excitation

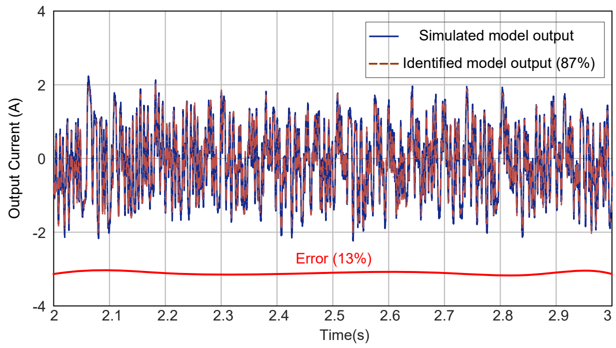

Fig.11. D-axis current outputs of simulation and identified model under the Q-axis voltage excitation

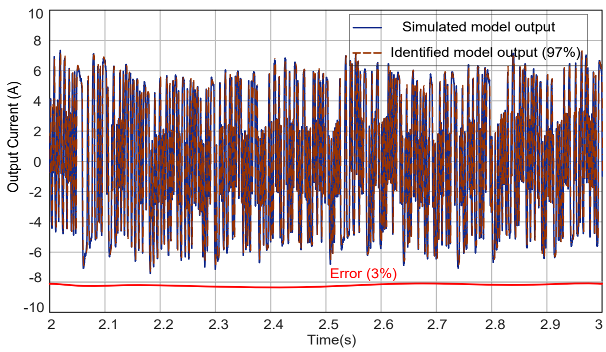

Fig.12. Q-axis current outputs of simulation and identified model under the Q-axis voltage excitation

B. Experiment Validation

In order to further verify the correctness of the proposed measurement method, a small-scale prototype based on the proposed impedance measurements setup, as shown in Fig.2, is built. However, in this setup, the shunt current injection method instead of the series voltage injection method was adopted because this method is much easier to implement for the experiment verification.

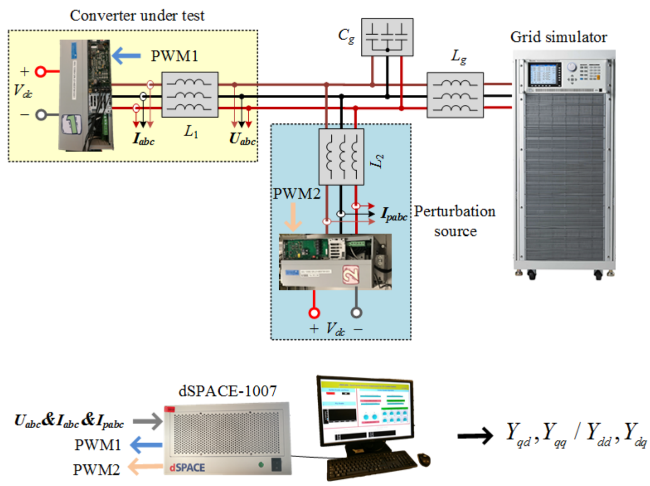

Fig.13. Small-scale prototype of the impedance measurement.

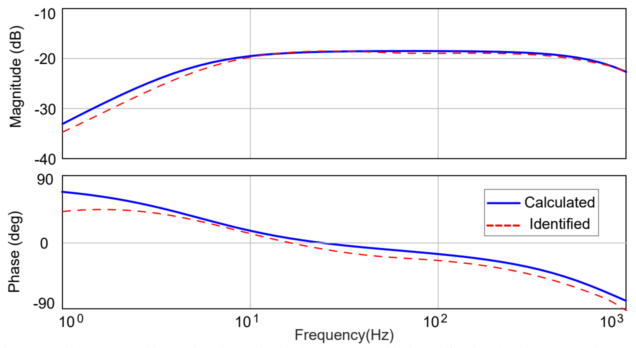

Fig.14. Theoretically calculated admittance and identified admittance of Y_{dd}.

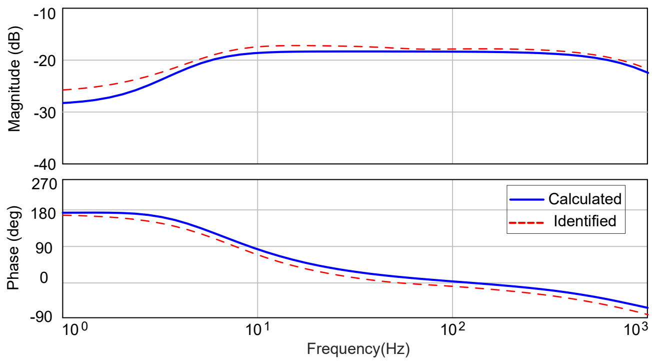

Fig.15.Theoretically calculated admittance and identified admittance of Y_{qq}.

Fig.13 shows the detailed experimental setup of the impedance measurement unit. A programmable three-phase voltage source is used to emulate the power gird. Two VSCs are used, where one is considered as the conveter under test, the other is used as the source of the perturbation. The current transducer LA 55-P and voltage transducer LV 25-P are used to acquire current and voltage signals for the calculation of the impedance. The sampled voltage and current are sent to the dSPACE and the synchronization phase was calculated based on the PLL and the voltage and current were recorded in the *dq*-domain.

In addition, the data would all be processed in the host computer and the impedance model would be identified based on recursive least squares algorithm.

Similarly, according to the experiment data, the parametric expression of the identified impedance model can be obtained. Nevertheless, since the coupling admittance Y_{dq}

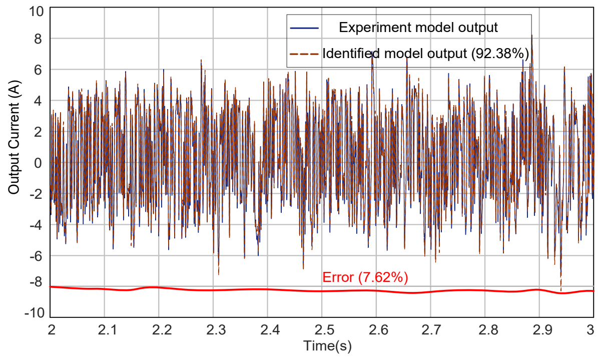

Fig.16. D-axis current outputs of experiment and identified model under the D-axis voltage excitation.

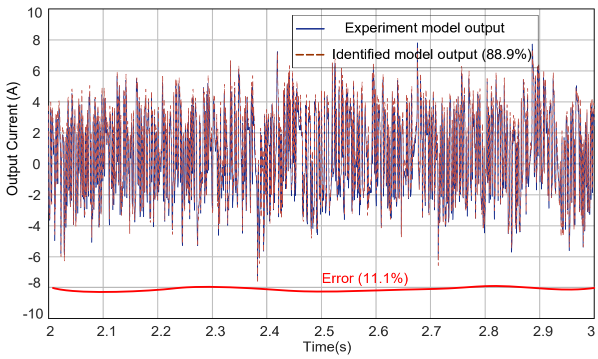

Fig.17. Q-axis current outputs of experiment and identified model under the Q-axis voltage excitation.

and Y_{qd} is relatively small, the current perturbation components would mostly flow into the grid impedance, which perturbs the coupling components of the converter slightly. Moreover, the noise in the experiment is more obvious than in the simulation, which makes the useful information applied for the identification of the coupling admittance submerge in the noise. Therefore, only the admittance Y_{dd} and Y_{qq} are given

$$Y_{dd}=\frac{-0.04756z^{-1}+0.0452z^{-2}-0.0335z^{-3}+0.0353z^{-4}}{1-1.399z^{-1}+1.117z^{-2}-1.303z^{-3}+0.587z^{-4}}$$

$$Y_{qq}=\frac{0.0015+0.038z^{-1}+0.02z^{-2}-0.02z^{-3}-0.03z^{-4}}{1-0.038z^{-1}-0.92z^{-2}-0.64z^{-3}+0.608z^{-4}}$$

Fig.14 and Fig.15 show the theoretically calculated admittance and identified admittance based on the experiment data. As can be seen, the identified admittance Y_{dd} and Y_{qq} match well with the theoretically calculated ones, which has proved the accuracy of the impedance measurement method based on the parametric identification. In addition, the accuracy of the identified impedance model is also verified in the time domain by using the recorded experiment data, as shown in Fig.16 and Fig.17. The compared results show that the impedance measurement results based on the parametric identification still match the theoretical impedance model very well (92.38% and 88.9%).

VI. Conclusions

This paper proposes the use of PRBS as injected perturbations for exciting the response of VSC, and the parametric expressions of the transfer function of the impedance model is identified based on recursive least squares algorithm. The compared results between the identified model and theoretical model show that the identified model matches very well with theoretical model. This study not only demonstrates the accuracy of the impedance measurement method based on the parametric identification which can be applied for stability analysis, but also provides a way to verify the correctness of the small-signal modelling methods of VSC.

References

[1] J. Sun, "Impedance-based stability criterion for grid-connected Inverters," IEEE *Trans. Power Electron.*, vol. 26, no. 11, pp. 3075-3078, Nov. 2011.

[2] W. Cao, Y. Ma, L. Yang, F. Wang and L. M. Tolbert, "D–Q impedance based stability analysis and parameter design of three-phase inverter-based AC power systems," *IEEE Trans. Ind. Electron.*, vol. 64, no. 7, pp. 6017-6028, July.2017.

[3] X.Feng, J. Liu and F. C. Lee, "Impedance specifications for stable DC distributed power systems", *IEEE Trans. Power Electron*., vol. 17, no. 2, pp. 157-162, Mar. 2002.

[4] A. Riccobono and E. Santi, "Comprehensive review of stability criteria for DC power distribution systems," *IEEE Trans. Ind. Appl.*, vol. 50, no.5, pp. 3525-3535, Oct. 2014.

[5] B. Wen, D. Boroyevich, R. Burgos, P. Mattavelli and Z. Shen, "Small-signal stability analysis of three-phase ac systems in the presence of constant power loads based on measured d-q frame impedances", *IEEE Trans. Power Electron.,* vol. 30, no. 10, pp. 5952-5963, Oct. 2015.

[6] J. Huang, K. A. Corzine and M. Belkhayat, "Small-signal impedance measurement of power-electronics-based AC power systems using line-to-line current injection", *IEEE Trans. Power Electron*., vol. 24, no. 2, pp. 445-455, Feb. 2009.

[7] G. Francis, R. Burgos, D. Boroyevich, F. Wang and K. Karimi, "An algorithm and implementation system for measuring impedance in the D-Q domain", in *Proc. Energy Convers. Congr. Expo* (*ECCE*). Sep. 2011, pp. 3221-3228.

[8] S. Neshvad, S. Chatzinotas and J. Sachau, "Wideband identification of power network parameters using pseudo-random binary sequences on power inverters", *IEEE Trans. Smart Grid*, vol. 6, no. 5, pp. 2293-2301, Sept. 2015.

[9] B. Zhou, M. Jacsic. "Small-signal impedance identification of three-phase diode rectifier with multi-tone injection", in *Proc. Appl. Power Electron. Conf. Expo*.(*APEC*), Mar. 2014, pp. 2746-2753.

[10] I, Rolf, M. Münchhof. "Identification of dynamic systems: an introduction with applications". *Springer Science & Business Media*, 2010.

[11] L. Arnedo, D. Boroyevich, R. Burgos and F. Wang, "Polytopic black-box modeling of dc-dc converters," in *Power Electron. Specialists Conf.*, Mar 2008, pp. 1015-1021.

[12] L. Arnedo, R. Burgos, D. Boroyevich and F. Wang, "System-level black-box DC-DC converter models," in *Proc. Appl. Power Electron. Conf. Expo*.(*APEC*), Mar. 2009, pp. 1476-1481.

[13] V. Valdivia, A. Lazaro, A. Barrado, P. Zumel, C. Fernandez and M. Sanz, "Black-box modeling of three-phase voltage source inverters for system-level analysis," *IEEE Trans. Ind. Electron*., vol. 59, no. 9, pp. 3648-3662, Sept. 2012.

[14] V. Valdivia, A. Lázaro, A. Barrado, P. Zumel, C. Fernández and M. Sanz, "Impedance identification procedure of three-phase balanced voltage source inverters based on transient response measurements," *IEEE Trans. Power Electron*., vol. 26, no. 12, pp. 3810-3816, Dec. 2011.

[15] G.Hugues, L.Wang, and P.C. Young. "Direct identification of continuous-time models from sampled data: Issues, basic solutions and relevance." *Identification of continuous-time models from sampled data. Springer*, London, 2008. 1-29.